Electromagnetic penetration depth and frequency-dependent optical conductivity for a proximity junction

W. Stephan and J. P. Carbotte
Physics Department, McMaster University, Hamilton, Ontario, Canada L8S 4M1
(Received 14 September 1990; revised manuscript received 13 December 1990)

We have calculated the electromagnetic penetration depth for the normal-metal side of a proximity junction including paramagnetic impurities in the strong-scattering model of Shiba and Rusinov. Pair breaking strongly affects the results and the low-temperature behavior is sensitive to the location of the states in the gap. We have also computed the frequency dependence of the optical conductivity and find structure in the gap on the normal-metal side which is similar to that found in the intrinsic case.

I. INTRODUCTION

One notable feature of the superconducting state is the almost complete screening of electromagnetic fields from the interior of bulk samples by surface supercurrents. For example, to a good approximation, an applied weak magnetic field decays exponentially in magnitude with distance into the superconductor, with a characteristic length λ which is called the electromagnetic penetration depth. For conventional bulk superconductors λ is only very weakly temperature dependent at low temperatures, with a rapid increase near the critical temperature where λ diverges. The general form of this temperature dependence is reasonably well described by the simple dependence predicted by the two-fluid model, $\lambda \propto [1-(T/T_c)^4]^{-1}$, so that the deviation of the temperature dependence from this form is often plotted. Recently, however, Kresin[1] has found that the penetration depth on the normal-metal side of a proximity-effect junction displays a rapid increase at low temperatures, in good agreement with experiment.[2-4]

The approach taken by Kresin[1] is to restrict the temperature range considered to only very low temperatures, where the penetration depth may be small compared to the coherence length and the film thickness d_N. Furthermore, the McMillan[5] model is used in the description of the proximity effect, requiring that the coherence length ξ be greater than the film thickness d_N. In this situation, Kresin finds that the standard result for the nonlocal (Pippard) limit penetration depth still holds, with the only concession to the proximity effect being the replacement of the BCS gap function by the gap function calculated within the McMillan[5] model. Consistent with this approach, paramagnetic impurities within the scheme of Shiba and Rusinov[6,7] (SR) may be included on the normal-metal side of the junction by including the appropriate self-energy contribution. We study this situation here.

The frequency dependence of the absorption of electromagnetic radiation by a superconductor is determined by the structure of the quasiparticle density of states,[8,9] and, as is the case for intrinsic superconductors with paramagnetic impurities,[6,7,10] optical experiments may be very useful in cases where the construction of good tunneling junctions is difficult for a particular material.

In this paper, the optical absorption of proximity-effect-induced superconductors will be considered. The conductivity is calculated in exactly the same manner as for the case of intrinsic superconductors, with, of course, the usual replacement of the gap function by the appropriate one. In Sec. II, we present the necessary formalism for the calculation of the penetration depth and results are given in Sec. III. In Sec. IV, we describe the optical conductivity with numerical results in Sec. V. Conclusions are to be found in Sec. VI.

II. FORMALISM FOR PENETRATION DEPTH

It is readily verified that Kresin's[1] final result [his Eqs. (16)–(19)] is unchanged, when magnetic impurities are introduced on the normal-metal side. Thus,

$$\lambda_N = \kappa \phi^{-1/3} , \tag{1a}$$

where

$$\kappa = 4(3^{-3/2}) \left[\frac{m^* v_{FN}}{12\pi^2 n e^2} \right]^{1/3} \tag{1b}$$

and

$$\phi = \pi T \sum_{m \geq 0} \frac{\Delta_N^2(m)}{\omega_m^2 + \Delta_N^2(m)} . \tag{1c}$$

In (1b), m^* and n are the effective mass and electron concentration in the film N, v_{FN} is the Fermi velocity in N, e is the electronic charge, and the Matsubara gap function $\Delta_N(m)$.

One further step required in the evaluation of the penetration depth is the familiar recasting of (1c) into the form of a real-frequency-axis integral, as our computer code solves for the function $\Delta_N(\omega)$ rather than the thermodynamic function $\Delta_N(m)$. Using the standard methods,[11] one finds

$$\phi = \tfrac{1}{2} \mathrm{Im} \int_0^\infty d\omega \frac{\Delta_N^2(\omega)}{\Delta_N^2(\omega) - \omega^2} \tanh(\beta\omega/2) . \tag{2}$$

Now (1) and (2), together with the gap equations, may be used to calculate the penetration depth of the normal-metal side of the junction including the effects of SR (Refs. 6 and 7) model impurities.

The gap equations involve four coupled equations for the four functions $\tilde{\Delta}_{S(N)}$ and $Z_{S(N)}$. On the real frequency axis, they are[11-15]

$$\tilde{\Delta}_S(\omega)=\Delta_{Ph}+\Gamma_S\tilde{\Delta}_N(\omega)/D_N(\omega)\ , \tag{3a}$$

$$Z_S(\omega)=1+\Gamma_S Z_N(\omega)/D_N(\omega)\ , \tag{3b}$$

$$\tilde{\Delta}_N(\omega)=\Gamma_N\tilde{\Delta}_S(\omega)/D_S(\omega)+\Gamma_2(\omega)\tilde{\Delta}_N(\omega)/D_N(\omega)\ , \tag{3c}$$

$$Z_N(\omega)=1+\Gamma_N Z_S(\omega)/D_S(\omega)+\Gamma_1(\omega)Z_N(\omega)/D_N(\omega)\ , \tag{3d}$$

where

$$D_1(\omega)=[\tilde{\Delta}_I^2(\omega)-\omega^2 Z_I^2(\omega)]^{1/2},\quad I=N \text{ or } S\ , \tag{3e}$$

with N normal and S superconductor. The square root in (3e) must always be chosen to have a positive real part.

The scattering rates Γ_S and Γ_N are parameters characteristic of the junction and will be given specific values here.

The frequency-dependent impurity scattering contributions Γ_1 and Γ_2 are given by[6,7,15]

$$\Gamma_1(\omega)=\frac{n_I}{2\pi N_{N0}}\sum_{l=1}^{\infty}(2l+1)(1-\eta_l\varepsilon_l)\times\frac{\omega^2 Z_N^2(\omega)-\tilde{\Delta}_N^2(\omega)}{\omega^2 Z_N^2(\omega)-\tilde{\Delta}_N^2(\omega)\varepsilon_l^2}\ , \tag{4a}$$

$$\Gamma_2(\omega)=\frac{n_I}{2\pi N_{N0}}\sum_{l=1}^{\infty}(2l+1)(\varepsilon_l-\eta_l)\varepsilon_l\times\frac{\omega^2 Z_N^2(\omega)-\tilde{\Delta}_N^2(\omega)}{\omega^2 Z_N^2(\omega)-\tilde{\Delta}_N^2(\omega)\varepsilon_l^2}\ , \tag{4b}$$

where the scattering parameters are

$$\varepsilon_l=\cos(\delta_l^+-\delta_l^-) \tag{5a}$$

and

$$\eta_l=\cos(\delta_l^++\delta_l^-)\ , \tag{5b}$$

with $\delta_l^{\pm}$ phase shifts. The impurity concentration n_I in Eq. (4) is sometimes given in terms of a parameter $\alpha=\pi n_I(1-\varepsilon_0^2)/mp_F$ with m the electron mass and p_F the Fermi momentum and we have in mind a single level in the gap given by ε_0. The value $\varepsilon_0=1$ corresponds to Abrikosov-Gorkov[10] theory (weak scattering).

The quantity Δ_{Ph} introduced in (3a) is the superconducting order parameter, which satisfies the usual BCS self-consistency equation

$$\Delta_{Ph}=N_{S0}V\int_0^{\omega_D}d\omega\,\mathrm{Re}\left[\frac{\tilde{\Delta}_S(\omega)}{[\omega^2 Z_S^2(\omega)-\tilde{\Delta}_S^2]^{1/2}}\right]\times\tanh(\beta\omega/2)\ , \tag{6}$$

where V is the pairing potential and N_{S0} is the density of electronic states on the superconducting side.

III. RESULTS FOR PENETRATION DEPTH

Kresin[1] has found that the zero-temperature penetration depth $\lambda(0)$ is an increasing function of the normal film thickness for a given superconducting film thickness, which is a result of the decrease of the strength of the superconducting correlations.

Considering the dependence of $\lambda(0)$ on paramagnetic impurity concentration, one finds that the results may be divided into two qualitatively different groups: In the one case $\Gamma_S<\Delta_0/2$, T_c and $\lambda(0)$ are finite for all values of Γ_N and α, and in the second case $\Gamma_S>\Delta_0/2$, critical values of Γ_N and α exist, for which T_c goes to zero and $\lambda(0)$ diverges. Some results for the first case are shown in Fig. 1(a), where the inverse penetration depth is plotted as a function of the pair-breaking parameter α (with the scattering parameter $\varepsilon_0=0$) for a few different values of Γ_N. The inverse of the penetration depth is plotted to avoid the divergence of $\lambda(0)$ which occurs at the critical concentration, and which shows up in the second case, Fig. 1(b), as the inverse penetration depth going to zero. Of course, long before this point is reached, the penetration depth will have increased to the point where it is of the order of the film thickness, which violates one of the

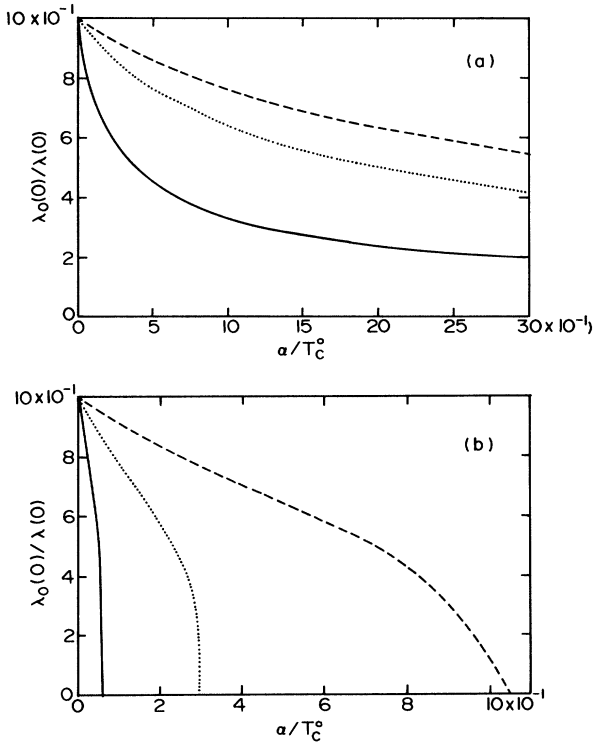

FIG. 1. The inverse electromagnetic penetration depth at zero temperature of the normal-metal side of a proximity-effect junction as a function of paramagnetic impurity concentration in the SR model with $\varepsilon_0=0$. (a) "Thick" superconducting film $\Gamma_S/T_c^0=0.36$ with T_c^0 the critical temperature in the absence of impurities, and $\Gamma_N/T_c^0=0.10$ (——), $\Gamma_N/T_c^0=0.72$ (· · · ·), $\Gamma_N/T_c^0=1.50$ (— — —). (b) "Thin" superconducting film $\Gamma_S/T_c^0=1.5$ and $\Gamma_N/T_c^0=0.36$ (——), $\Gamma_N/T_c^0=0.72$ (· · · ·), $\Gamma_N/T_c^0=1.50$ (— — —).

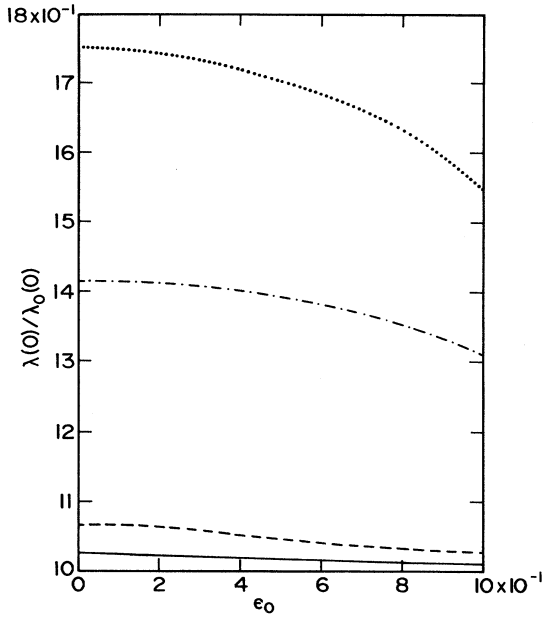

FIG. 2. The dependence of the zero-temperature penetration depth of the normal-metal side of a proximity-effect junction on the SR scattering parameter ε_0 for the parameters $\Gamma_N/T_c^0=0.72$; and $\Gamma_S/T_c^0=1.5$ and $\alpha/T_c^0=0.01$ (——), $\Gamma_S/T_c^0=1.5$ and $\alpha/T_c^0=0.20$ (· · · ·), $\Gamma_S/T_c^0=0.36$ and $\alpha/T_c^0=0.10$ (— — —), $\Gamma_S/T_c^0=0.36$ and $\alpha/T_c^0=0.72$ (—·—·—·).

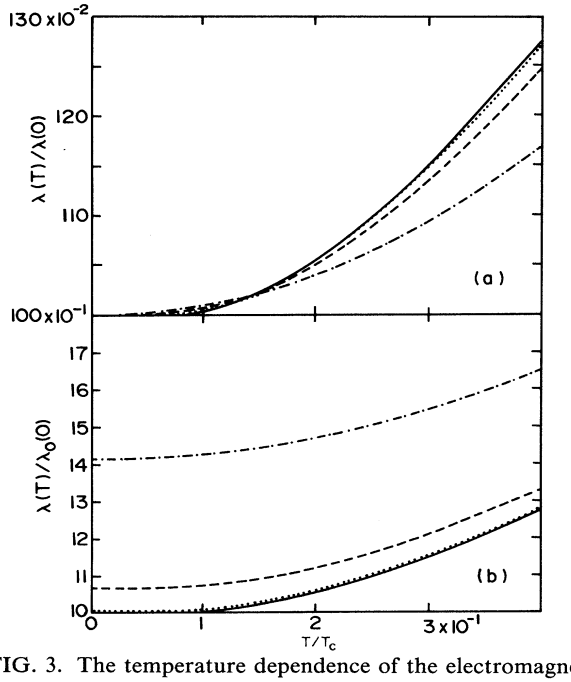

FIG. 3. The temperature dependence of the electromagnetic penetration depth of the normal-metal side of a proximity-effect junction containing SR model paramagnetic impurities. (a) The penetration depth $\lambda(T)$, normalized to the zero-temperature value $\lambda(0)$ for the same material, with parameters $\Gamma_S/T_c^0=0.36$, $\Gamma_N/T_c^0=0.72$, $\varepsilon_0=0$; and $\alpha/T_c=0$ (——), $\alpha/T_c=0.01$ (· · · ·), $\alpha/T_c=0.10$ (— — —), $\alpha/T_c=0.72$ (—·—·—·). (b) The penetration depth $\lambda(T)$ normalized to the zero-temperature value of the junction without paramagnetic impurities $\lambda_0(0)$ for the same parameters as in (a).

basic assumptions made at the outset. The large impurity concentration region is therefore not of interest within this model, although just what is large can only be decided after estimating the various parameters for a particular junction composition.

The dependence of $\lambda(0)$ on the Shiba-Rusinov scattering parameter ε_0 is explored in Fig. 2, where it is shown that as ε_0 increases $\lambda(0)$ decreases, with the amount of variation being larger for thin superconducting films (Γ_S large) and for larger impurity concentrations.

Next, consider the temperature dependence of the penetration depth, some examples of which are shown in Fig. 3(a), where the penetration depth, normalized to the zero-temperature value $\lambda(0)$, is plotted as a function of reduced temperature T/T_c. Note that with increasing impurity concentration, the rapid rise in λ at low temperature found in the pure case is suppressed. The mechanism for this may be better understood by examining Fig. 3(b), where the same results are replotted with a different normalization, that is with all values normalized to $\lambda_0(0)$, the penetration depth of the pure junction at zero temperature, rather than to $\lambda(0)$, the penetration depth at zero temperature for the given set of material parameters. When all curves are normalized by the same value, the actual shape of the curves at higher temperatures

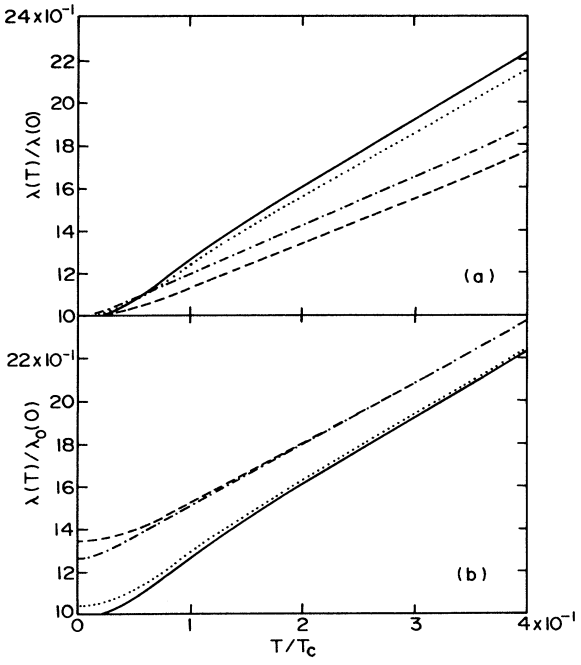

FIG. 4. The temperature dependence of the electromagnetic penetration depth of the normal-metal side of a proximity-effect junction containing SR model paramagnetic impurities. (a) The penetration depth $\lambda(T)$, normalized to the zero-temperature value $\lambda(0)$ for the same material, with parameters $\Gamma_S/T_c^0=0.36$, $\Gamma_N/T_c^0=0.10$; and $\alpha/T_c=0$ (——), $\alpha/T_c=0.01$ and $\varepsilon_0=0$ (· · · ·), $\alpha/T_c=0.10$ and $\varepsilon_0=0$ (— — —), $\alpha/T_c=0.10$ and $\varepsilon_0=1.0$ (—·—·—·). (b) The penetration depth $\lambda(T)$ normalized to the zero-temperature value of the junction without paramagnetic impurities $\lambda_0(0)$ for the same parameters as in (a).

($T/T_c \simeq 0.3-0.4$) is not greatly affected by increasing α; to a good approximation in this region the curves simply shift up by a constant amount. At lower temperatures, the shape of the curves is altered slightly, with the increase in $\lambda(T)/\lambda_0(0)$ with α being largest at zero temperature. The marked decrease in slope of the curves in Fig. 3(a) at higher temperatures with increasing α simply reflects the fact that the low-temperature penetration depth increases more rapidly than that at higher temperatures.

The usefulness of the above pictorial display becomes most evident upon consideration of the dependence of these results on the scattering parameter ε_0, an example of which is shown in Fig. 4. Although the curves for $\varepsilon_0=0$ and for $\varepsilon_0=1.0$ differ markedly in Fig. 4(a) at all temperatures, the results plotted in Fig. 4(b) show that in absolute terms only at the very lowest temperatures does the value of ε_0 have any effect. This is reassuring, as for the parameters considered here the parameter ε_0 affects only the very low frequency region of the gap function, so that one would expect only the very low-temperature region to be influenced by this parameter.

In summary, the low-temperature penetration depth of the normal-metal side of a proximity-effect junction has been found to be sensitive to the introduction of paramagnetic impurities. The rapid rise of penetration depth with temperature reported by Kresin[1] for the case of a pure proximity junction is found to be suppressed by paramagnetic impurities, an effect which results from λ in the very low-temperature region being more strongly enhanced than at higher temperatures. Furthermore, this low-temperature enhancement is quite sensitive to the nature of the impurity scattering as described by the parameter ε_0.

IV. FORMALISM FOR CONDUCTIVITY

The optical absorption of the normal side (N) of a proximity junction is given by[8-9,16,17]

$$\frac{\sigma_1(\omega)}{\sigma_N}=\frac{1}{\omega}\int_{\omega_g-\omega}^{\omega_g} d\nu[n(\nu)n(\omega+\nu)+p(\nu)p(\omega+\nu)]\tanh\left[\frac{\beta}{2}(\omega+\nu)\right]+\frac{1}{\omega}\int_{\omega_g}^{\infty} d\nu[n(\nu)n(\omega+\nu)+p(\nu)p(\omega+\nu)]\times\left[\tanh\left[\frac{\beta}{2}(\omega+\nu)\right]-\tanh\left[\frac{\beta\nu}{2}\right]\right]. \tag{7}$$

Here,

$$n(\nu)=\mathrm{Re}\left[\frac{\nu}{[\nu^2-\Delta_N^2(\nu)]^{1/2}}\right] \tag{8a}$$

is the single particle density of states, and

$$p(\nu)=\mathrm{Re}\left[\frac{\Delta_N(\nu)}{[\nu^2-\Delta_N^2(\nu)]^{1/2}}\right] \tag{8b}$$

is the pair density of states. Here σ_N is the normal state conductivity and is assumed to be frequency independent in the frequency range of interest. The frequency ω_g is the lowest frequency where the density of states becomes nonzero. Equation (7) can be integrated numerically, once the solution for the gap equations for $\Delta_N(\omega)$ on the normal side is known.

The normal side gap appearing in Eqs. (7) and (8) follows from Eq. (3), which can be rewritten in the form

$$\Delta_N(\omega)=\frac{\Gamma_N\Delta_S(\omega)}{[\Delta_N^2(\omega)-\omega^2]^{1/2}}\left[1+\frac{\Gamma_N}{[\Delta_S^2(\omega)-\omega^2]^{1/2}}+\frac{\Gamma(\omega)}{[\Delta_N^2(\omega)-\omega^2]^{1/2}}\right]^{-1} \tag{9a}$$

and

$$\Delta_S(\omega)=\left[\Delta_{Ph}+\frac{\Gamma_S\Delta_N(\omega)}{[\Delta_N^2(\omega)-\omega^2]^{1/2}}\right]\times\left[1+\frac{\Gamma_S}{[\Delta_N^2(\omega)-\omega^2]^{1/2}}\right]^{-1}. \tag{9b}$$

The frequency-dependent pair-breaking parameter in (9a)

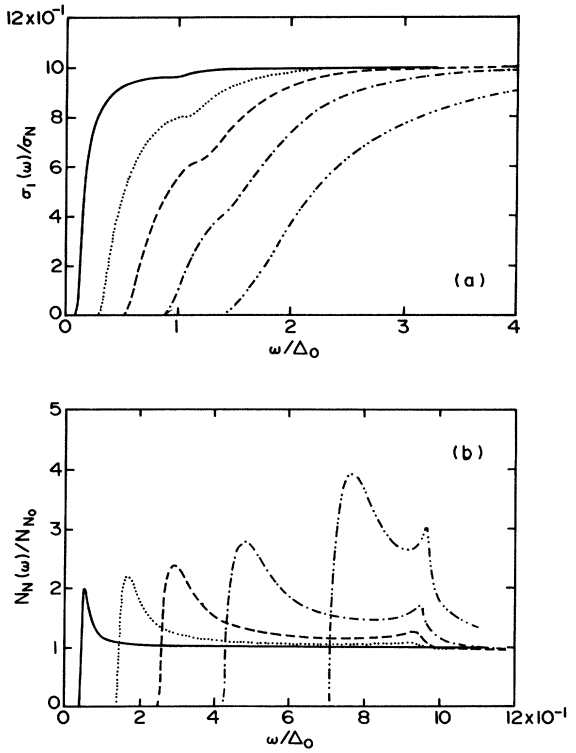

FIG. 5. (a) The frequency dependence of the optical absorption (in units of the unperturbed gap Δ_0) of the normal-metal side of a pure proximity-effect junction with a thick superconducting film $\Gamma_S/T_c^0=0.1$ and for $\Gamma_N/T_c^0=0.10$ (——), $\Gamma_N/T_c^0=0.36$ (· · · ·), $\Gamma_N/T_c^0=0.72$ (— — —), $\Gamma_N/T_c^0=1.50$ (—·—·—·), $\Gamma_N/T_c^0=4.00$ (—··—··—). (b) The density of states of the normal-metal side of a junction $N_N(\omega)/N_0$ for the same parameters as in (a).

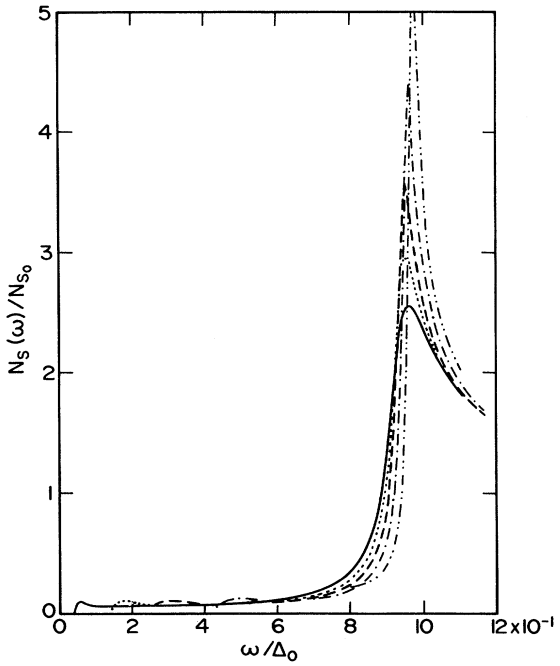

FIG. 6. The density of states of the superconducting side of a proximity-effect junction for the same parameters as in Fig. 1.

is given for Shiba-Rusinov impurities, by

$$\Gamma(\omega)=\frac{n_I}{2\pi N_{N0}}\sum_{l=1}^{\infty}(2l+1)(1-\varepsilon_l^2)\frac{\omega^2-\Delta_N^2(\omega)}{\omega^2-\Delta_N^2(\omega)\varepsilon_l^2}\ . \quad (10)$$

In the Arikosov-Gorkov[10,18] limit $\varepsilon_0\to 1$, in which case Γ is frequency independent.

V. NUMERICAL RESULTS FOR CONDUCTIVITY

First, considering the variation of the absorption with normal film thickness without paramagnetic impurities, one might expect this to be very much like that of a BCS superconductor, with a gap edge that decreases with increasing normal film thickness d_N. [Note that $\Gamma_S/\Gamma_N=(d_N/d_S)(N_{N0}/N_{S0})$]. This is indeed the case to a reasonably good approximation, as shown in Fig. 5(a), although there is a small kink in the curves at a frequency which depends on the film thickness. This feature is associated with the two-peaked structure of the density of states, shown in Fig. 5(b) (the densities of states on the superconducting side are shown in Fig. 6 for the sake of completeness). In the two extreme limits of Γ_N going to zero or infinity, the two-peaked structure disappears, in the one case, because the density of states becomes identical to that of the normal state, and in the other case, be-

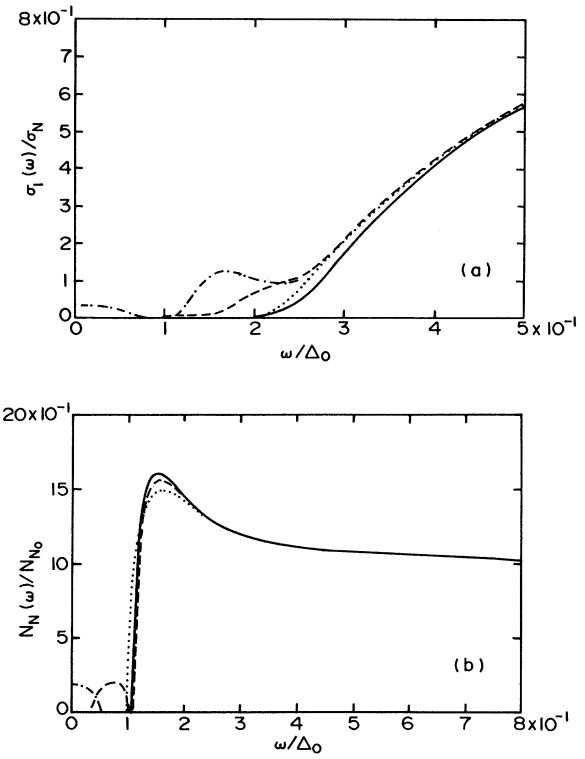

FIG. 7. The frequency dependence of the optical absorption of the normal-metal side of a proximity-effect junction containing a small amount of SR paramagnetic impurities $\alpha/T_c^0=0.01$, for $\Gamma_S=\Gamma_N=0.36T_c^0$ and $\varepsilon_0=1.0$ (· · · ·), $\varepsilon_0=0.5$ (— — —), $\varepsilon_0=0.0$ (—·—·—·). Also included is the pure case $\alpha=0$ (——). (b) The density of states on the normal-metal side of the junction for the same parameters as in (a).

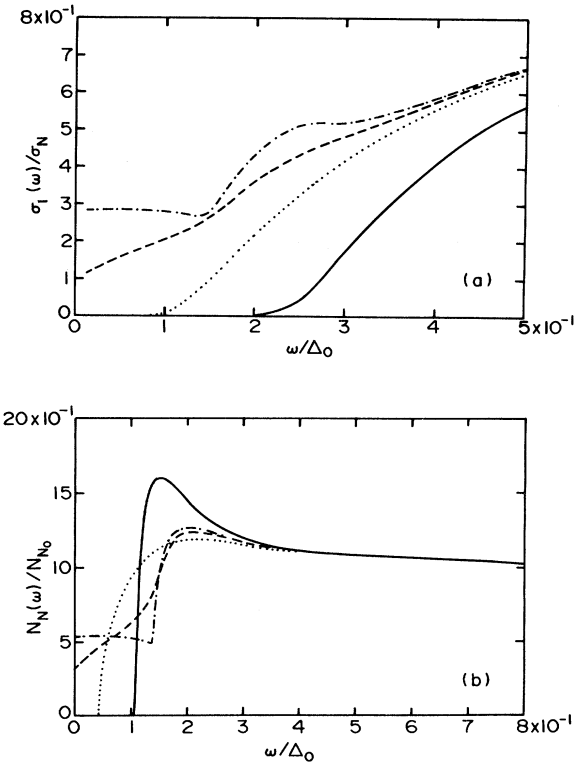

FIG. 8. (a) The frequency dependence of the optical absorption of the normal-metal side of a proximity-effect junction containing a small amount of SR paramagnetic impurities, $\alpha/T_c^0=0.1$, for $\Gamma_S=\Gamma_N=0.36T_c^0$ and $\varepsilon_0=1.0$ (· · · ·), $\varepsilon_0=0.5$ (— — —), $\varepsilon_0=0.0$ (—·—·—·). Also included is the pure case $\alpha=0$ (——). (b) The density of states on the normal-metal side of the junction for the same parameters as in (a).

cause the two peaks merge together into a single one. The structure is most evident in the intermediate thickness cases of Fig. 5(a). Although this structure is easily seen in some of the calculated curves, it is questionable as to whether or not it might be seen experimentally. The densities of states calculated within the present model represent an idealized version of what is observed experimentally where structures are generally not as sharp as the calculated ones. This might well result in this feature becoming unobservably small for real systems.

Turning now to the question of including paramagnetic impurities in the normal-metal side of the junction, it has previously been pointed out by Kaiser[19] for the model of Müller-Hartmann and Zittartz,[20–22] which is very similar to that of Shiba[6] and Rusinov,[7] that the location of states within the energy gap is quite well described by the nonproximity results, with the replacement of the order parameter by an effective gap given by the location of the peak in the density of states in the absence of impurities. In light of this, it should not be surprising to see that the low frequency region of the optical absorption is very similar to that of the intrinsic case considered in our previous paper.[9] Figures 7 and 8 show a comparison of results for the scattering parameters $\varepsilon_0=0.0$, 0.5, and 1.0 for two different exchange scattering rates α. Note that the existence of a band of states in the gap leads to two peaks in the optical absorption, just as in the intrinsic case. The absorption at higher frequencies is not very sensitive to small amounts of paramagnetic impurities.

In conclusion, just as in the case of intrinsic superconductors, optical absorption is a very sensitive probe of the density of states of induced superconductors, and as such may be a useful tool in the probing of the interactions between magnetic impurities and conduction electrons in metals in general.

VI. CONCLUSION

The electromagnetic penetration depth at low temperature is found to be quite sensitive to the addition of paramagnetic impurities, with the rapid rise with increasing temperature found by Kresin[1] in the pure case being suppressed with increasing pair breaking. The low-temperature penetration depth is also shown to be sensitive to the location of the states in the gap determined by the SR scattering parameter ε_0.

The optical absorption of the normal-metal side of a proximity-effect junction is found to have a small structure associated with the two-peaked structure of the density of states predicted by the McMillan model, although this may not be observable experimentally. The addition of SR model paramagnetic impurities to the normal-metal side of a proximity-effect junction results in optical absorption which is qualitatively the same as that of the intrinsic case.

[1] V. Kresin, Phys. Rev. B **32**, 145 (1985).
[2] R. Simon and P. Chaikin, Phys. Rev. B **23**, 4463 (1981); **30**, 3750 (1984).
[3] R. Simon, P. Chaikin, and S. Wolf, Bull. Amer. Phys. Soc. **27**, 205 (1982).
[4] A. Mota, D. Marek, and J. Weber, Helv. Phys. Acta **55**, 647 (1982).
[5] W. L. McMillan, Phys. Rev. **175**, 537 (1968).
[6] H. Shiba, Prog. Theor. Phys. **40**, 435 (1968).
[7] A. I. Rusinov, Zh. Eksp. Teor. Fiz. **56**, 2043 (1969) [Sov. Phys.—JETP **29**, 1101 (1969)].
[8] J. Schrieffer, *Theory of Superconductivity* (Benjamin, New York, 1964).
[9] W. Stephan and J. P. Carbotte, Phys. Rev. B **33**, 4615 (1986); **34**, 4897(E) (1986).
[10] A. A. Abrikosov and L. P. Gorkov, Zh. Eksp. Teor. Fiz. **39**, 1781 (1960) [Sov. Phys.—JETP **12**, 1243 (1961)].
[11] A. B. Kaiser and M. J. Zuckermann, Phys. Rev. B **1**, 229 (1970).
[12] A. B. Kaiser, Phys. Rev. B **22**, 2323 (1980).
[13] K. Machida, J. Low Temp. Phys. **27**, 737 (1977).
[14] K. Machida and L. Dumoulin, J. Low Temp. Phys. **31**, 143 (1978).
[15] M. B. Maple, in *Magnetism*, edited by G. T. Rado and H. Suhl (Academic, New York, 1973), Vol. 5, p. 289.
[16] S. B. Nam, Phys. Rev. **156**, 487 (1967).
[17] K. Machida, Prog. Theor. Phys. **54**, 1251 (1975).
[18] M. B. Maple, Ref. 15.
[19] A. B. Kaiser, Phys. Rev. B **22**, 2323 (1980).
[20] J. Zittarz and E. Müller-Hartmann, Z. Phys. **232**, 11 (1970).
[21] E. Müller-Hartmann and J. Zittarz, Z. Phys. **234**, 58 (1970).
[22] J. Zittarz, Z. Phys. **237**, 419 (1970).